JOURNAL OF VIROLOGY, Dec. 1979, p. 968-978
0022-538X/79/12-0968/11$02.00/0

Vol. 32, No. 3

Genome Organization of Retroviruses

VI. Heteroduplex Analysis of Ecotropic and Xenotropic Sequences of Moloney Mink Cell Focus-Inducing Viral RNA Obtained from Either a Cloned Isolate or a Thymoma Cell Line

ROBERT A. BOSSELMAN, LEO J. L. D. VAN GRIENSVEN,† MARGUERITE VOGT, AND INDER M. VERMA*

Tumor Virology Laboratory, The Salk Institute, San Diego, California 92112

Received for publication 29 May 1979

The genome of a recombinant murine leukemia virus capable of inducing focal areas of morphological alteration in mink lung fibroblasts was studied by heteroduplex analysis. The dual-tropic recombinant virus was isolated from a thymoma cell line ($Th_{16.3}$) and is referred to as BALB/Moloney mink cell focus-inducing virus (BALB/Mo-MCF virus). The nucleic acid sequences of RNA from virions obtained from either a thymoma cell line ($Th_{16.3}$) or a clonal isolate (BALB/Mo-MCF_{81}) were compared with the genomes of ecotropic and xenotropic viruses. The following inferences were drawn (i) A single nonhomologous region (substitution loop α) of about 0.7 kilobase was observed in a heteroduplex formed between Moloney murine leukemia virus complementary DNA (cDNA) and BALB/Mo-MCF_{81} RNA. This nonhomology region was mapped between 1.71 and 2.40 kilobases from the 3′ end of the genome. (ii) The predominant class of heteroduplexes formed between virion RNA obtained from the thymoma cell line ($Th_{16.3}$) and Moloney murine leukemia virus cDNA showed a substitution loop similar to that observed with the RNA obtained from a cloned isolate, BALB/Mo-MCF_{81}. However, there were other molecules with additional regions of nonhomology. (iii) Heteroduplexes formed between NZB xenotropic RNA and ecotropic Moloney murine leukemia virus cDNA exhibited four major nonhomology regions extending 0.75 to 1.46, 2.0 to 2.8, 3.6 to 4.3, and 7.4 to 7.9 kilobases from the 3′ end of the genome. (iv) The MCF-specific substitution loop α (1.71 to 2.40 kilobases) appeared as a duplex region when NZB xenotropic RNA was hybridized to cDNA transcripts synthesized by virions obtained from thymoma cell line $Th_{16.3}$. The position of the other substitution loops observed in a heteroduplex formed between NZB xenotropic RNA and Moloney murine leukemia virus cDNA was not affected. (v) Heteroduplexes formed between xenotropic BALB virus 2 cDNA and NZB xenotropic RNA demonstrated a large degree of nucleic acid sequence homology. Of the 29 heteroduplexes examined, 24 appeared to be homoduplexes, and in the remaining 5 heteroduplexes only one region of nonhomology located between 3.2 and 3.8 kilobases from the 3′ end of the genome could be identified. Hybridization of BALB virus 2 xenotropic RNA to NZB xenotropic cDNA followed by digestion with single-strand-specific nuclease S1 showed an 80% sequence homology.

Murine leukemia viruses (MLVs) may be classified into three major groups: (i) ecotropic viruses, which replicate in rodent cells but are restricted for growth in cells of other species (16); (ii) xenotropic viruses, which are unable to grow in mouse cells but are capable of replication in nonmurine cells (3, 23); and (iii) amphotropic viruses, which are unrestricted for growth in cells of either murine or nonmurine origin (17, 24). Recently, mink cell focus-inducing (MCF) viruses have been described which have a dual host range similar to that of the amphotropic viruses. However, their growth is not interfered with by amphotropic viruses, but it is interfered with by ecotropic and xenotropic viruses (14, 15, 18, 30). These dual-tropic MCF MLVs induce focal areas of morphological alteration in mink lung fibroblasts and have been implicated as playing a key role in the genesis of spontaneous

† On leave of absence from the Department of Experimental Pathology, Erasmus University, Rotterdam, The Netherlands.

lymphomas (18) and leukemias (29).

The MCF MLVs appear to have arisen by recombination between ecotropic and xenotropic envelope genes. Three kinds of biochemical studies support this notion. (i) Tryptic peptide analyses of the major envelope glycoprotein, gp70, from several isolates of MCF MLVs show peptides in common with both xenotropic and ecotropic gp70's (8, 30). (ii) RNase T1 oligonucleotide mapping of several MCF RNAs show that MCF-specific oligonucleotides are clustered in the 3′ half of the genome encompassing the *env* gene (10, 25, 26). (iii) Heteroduplexes formed between several MCF RNAs and parental ecotropic complementary DNA (cDNA) transcripts show a nonhomology region of about 0.7 to 0.8 kilobase (kb) located in the envelope gene (6, 7). Thus, it appears that MCF viruses are ecotropic MLVs which have acquired some sequences of their envelope gene from xenotropic viruses.

Vogt (32) recently has described the biological properties of MCF viruses isolated from thymoma lines of BALB/Mo mice. This mouse strain is derived from a BALB/c 129J preimplantation embryo infected with Moloney MLV (Mo-MLV). In this BALB/Mo strain, Mo-MLV is transmitted as a single Mendelian gene (21, 22). Like the other MCF MLVs, BALB/Mo-MCF virus also exhibits a dual host range and appears to have arisen by recombination within the envelope gene between ecotropic (NB-tropic) Mo-MLV and xenotropic MLV. We report here the nucleic acid sequence relationships of both a cloned isolate of BALB/Mo-MCF virus (BALB/Mo-MCF_{81}) and virus obtained from a primary tumor line ($Th_{16.3}$) to their parental ecotropic virus. In an effort to establish the origin of xenotropic sequences present in BALB/Mo-MCF virus, we have compared its nucleic acid sequences with the genomes of xenotropic BALB virus 2 (BALB-2) and xenotropic NZB virus. Furthermore, the sequence relationship of the two xenotropic viruses has also been investigated. These studies were carried out by heteroduplex analysis, a technique which involves the formation of hybrids between genome-length viral cDNA transcripts and viral genomic RNA. The hybrids are then analyzed by electron microscopy. The results indicate the following. (i) There is a region of nonhomology between the cloned BALB/Mo-MCF_{81} and Mo-MLV extending 1.7 to 2.4 kb from the 3′ end of the genome. The principal region of nonhomology between BALB/Mo-MCF RNA obtained from the primary tumor cell line and Mo-MLV cDNA also extends from 1.7 to 2.4 kb. However, there are other molecules with additional regions of nonhomology. (ii) There are four major regions of nonhomology between NZB virus and Mo-MLV extending 0.75 to 1.46, 2.0 to 2.8, 3.6 to 4.3, and 7.4 to 7.9 kb from the 3′ end of the genome. (iii) The MCF-specific region of nonhomology (1.7 to 2.4 kb) appears as a duplex region when xenotropic NZB RNA is hybridized to cDNA synthesized from virions obtained from the primary tumor. (iv) There is a large degree of sequence homology between the two xenotropic viruses. The only region of nonhomology between the BALB-2 and NZB genomes is located between 3.2 and 3.8 kb from the 3′ end of the genome. Hybridization of BALB-2 RNA to NZB cDNA shows a sequence homology of about 80%.

MATERIALS AND METHODS

Cells and viruses. All cells were grown in Dulbecco-Vogt-modified Eagle medium supplemented with 10% fetal calf serum. Mo-MLV clone 1 was obtained from H. Fan and was grown as described previously (12).

Mo-MLV clone E7. SC-1 cells were infected with supernatant fluid obtained from cultured BALB/Mo thymoma cells ($Th_{16.3}$) at an average multiplicity of infection of 2.2. At 6 h postinfection, single cells were isolated for cloning. Clone E7 is XC-positive and has no cytopathic effects on either mouse or mink cells. Like Mo-MLV clone 1, it is also NB tropic.

$Th_{16.3}$. The $Th_{16.3}$ cell line was derived from a spontaneous thymoma of BALB/Mo mice (21, 22). The cells carry the antigen (R. Hyman, personal communication) and produce both Mo-MLV and Mo-MCF virus (32).

Thymoma $MPV_{11.1}$. A cloned cell line derived from a thymoma of a D2 new × 129J F1 mouse infected with Moloney plasma virus (MPV) as a newborn was kindly provided by R. Hyman. The cells produce both Mo-MLV and Mo-MCF virus. The biological properties of Mo-MCF virus isolated from this cell line ($MPV_{11.1}$) are indistinguishable from those of Mo-MCF_{81} (M. Vogt, personal communication).

BALB/c Mo-MCF virus (BALB/Mo-MCF_{81}. A cloned isolate was propagated on mink lung cells which were infected with biologically purified Mo-MCF virus isolated from $Th_{16.3}$ cells (32).

NZB xenotropic virus. Spontaneously released endogenous xenotropic virus from NZB mice was obtained from F. Jensen, Scripps. Clinic, and propagated in rabbit lung endothelial cell line 179.

BALB-2. BALB-2 was obtained through the Office of Program Resources and Logistics, Viral Cancer Program, National Cancer Institute. It was isolated from Fisher rat cells as a mixture of BALB-2 and Kirsten mouse sarcoma virus (BALB V2) pseudotype virus. It is referred to as BC·169-BALB V-2 (lot 5003, 32–56). The virus was tested in our laboratory for its xenotropic host range. It was found to grow in mink lung cells but not in SC-1 cells, as assayed by reverse transcriptase activity. The 35S helper virus RNA was separated from Kirsten mouse sarcoma virus by sedimentation on sucrose gradients.

Synthesis of long cDNA transcripts. Essentially the conditions described previously (31) were used. The total cDNA synthesized was fractionated on alkaline sucrose gradients, and material sedimenting at 19S to 20S (~8 to 9 kb) was recovered. The nucleic acids were precipitated (without addition of carrier) by high-speed centrifugation and stored as dry pellets at −20°C.

Preparation of viral RNA. The 60S to 70S RNA was prepared as described previously (11, 13), and the 35S RNA was prepared by heat denaturation of 60S to 70S RNA (20). Briefly, 60S to 70S RNA was precipitated with ethanol and dissolved in 0.01 M Tris-hydrochloride (pH 7.4)–0.1 M NaCl–0.001 M EDTA–0.1% sodium dodecyl sulfate (TNE buffer) and heat denatured by boiling for 2 min, which was followed by quenching on ice. The RNA was then fractionated on 15 to 30% sucrose gradients made in TNE buffer. Material sedimenting between 35S and 38S was collected, and nucleic acid was recovered by high-speed centrifugation without addition of carrier nucleic acids for co-precipitation.

Hybridization. [^{3}H]cDNA was synthesized in an endogenous reaction by using denatured calf thymus DNA (2 mg/ml) as primer (28). The standard hybridization mixture contained about 3,000 cpm of ^{3}H-labeled NZB cDNA and 0.1 μg of viral RNA in 5 μl of buffer containing 0.01 M TES [*N*-tris(hydroxymethyl)methyl-2-aminoethanesulfonic acid], pH 7.5, 0.6 M NaCl, and 0.001 M EDTA. Hybridizations were performed at 68°C to a C_rt of ≥ 10, and the hybrids were scored by resistance to single-strand-specific nuclease S1, as described previously (31).

Heteroduplex formation and electron microscopy. Full-length cDNA (1.5 μg/ml) and genomic 35S to 38S viral RNA (1 μg/ml) were incubated at 49°C for 30 min in 10 μl of a solution containing 0.01 M PIPES [piperazine-*N*,*N*′-bis(2-ethanesulfonic acid], 0.4 M NaCl, 0.001 M EDTA, and 80% formamide, pH 6.3 (6). To identify the 3′ ends of the RNA, 3-μl samples were adjusted to contain 0.01 M TES and 20% formamide in 10 μl and were incubated for 10 min at room temperature with circular polyoma DNA containing covalently attached polydeoxybromouridylic acid (2, 6).

Heteroduplexes were adsorbed to Parlodion-coated grids, stained with uranyl acetate, shadowed with platinum-carbon, and examined in a Hitachi Hu-11B transmission electron microscope. Selected molecules were photographed at a magnification of ×10,000. Contour lengths determined with a Hewlett-Packard digitizer.

Molecular lengths expressed in kilobases were determined by comparison with double-stranded polyoma DNA and single-stranded φX 174 DNA spread under identical conditions. The length ratio of double-stranded to single-stranded DNA was 1:1.11.

RESULTS

Localization of MCF-specific region. (i) Mo-MLV cDNA-BALB/Mo-MCF$_{81}$ RNA. Long Mo-MLV cDNA transcripts were hybridized to cloned Mo-MCF RNA. Figure 1A shows a linear heteroduplex. The only region of sequence nonhomology between the two viral genomes is a substitution loop α (Fig. 1A, arrows). The 3′ end of the heteroduplex in Fig. 1A is determined by hybridizing the polyadenylic acid moiety of Mo-MCF RNA to polyoma viral DNA containing deoxybromouridine tails (6). The substitution loop α is 0.7 ± 0.18 kb long. It extends 1.71 ± 0.33 to 2.40 ± 0.30 kb from the 3′ end of the genome. The length of the long duplex region shown in Fig. 1A is about 5.9 ± 1.2 kb. The length of the longer duplex arm depended on the size of the cDNA transcripts and Mo-MCF RNA. Thus, nonhomology regions in close proximity to the 5′ end of the genome cannot be ruled out. About 25% of the heteroduplexes examined spanned the entire genome (9.0 kb).

Figure 1B shows a circular heteroduplex formed between Mo-MLV cDNA and Mo-MCF RNA. Because of terminal redundancy of the genomic RNA and initiation of cDNA synthesis at the 5′ end of the genome (27) followed by chain elongation at the 3′ end, the cDNA transcript is a circular permutation of viral RNA. Thus, a circular heteroduplex can be generated by hybridization of genome-length RNA to long cDNA transcripts (20). As in the case of linear heteroduplexes, only one substitution loop with similar coordinates can be seen. The remainder of the heteroduplex appears to be double stranded. The formation of circular heteroduplexes suggests that the sequences near the 5′ ends of the two RNAs are homologous.

Figure 1C shows a histogram depicting the extent and frequency of the substitution loop found in the Mo-MLV cDNA–Mo-MCF RNA heteroduplexes. The two arms of the substitution loop α appear to be of different lengths. It has been noted previously (6) that under 60% formamide spreading conditions, RNA is more condensed than single-stranded cDNA transcripts and therefore appears shorter. The data presented here represent the longer arm of the substitution loop. The average size of the substitution loop appears to be about 700 nucleotides, which is in general agreement with that described for AKR MCF, Mo-MCF$_{83}$, and HIX virus RNAs (6, 7).

(ii) Mo-MLV cDNA-virion RNA obtained from thymoma cell line Th$_{16.3}$. The heteroduplexes shown in Fig. 1 were obtained by using viral RNA from a cloned isolate, Mo-MCF$_{81}$. This clonal isolate was obtained by cocultivating cells from a BALB/Mo thymoma line (Th$_{16.3}$) with mink lung cells and by subsequently passing the virus yield through several cycles of infection at limiting dilution (alternately through mink lung and wild mouse [SC-1] cells) (32). This procedure successfully eliminates the vast excess of ecotropic virus present in BALB/

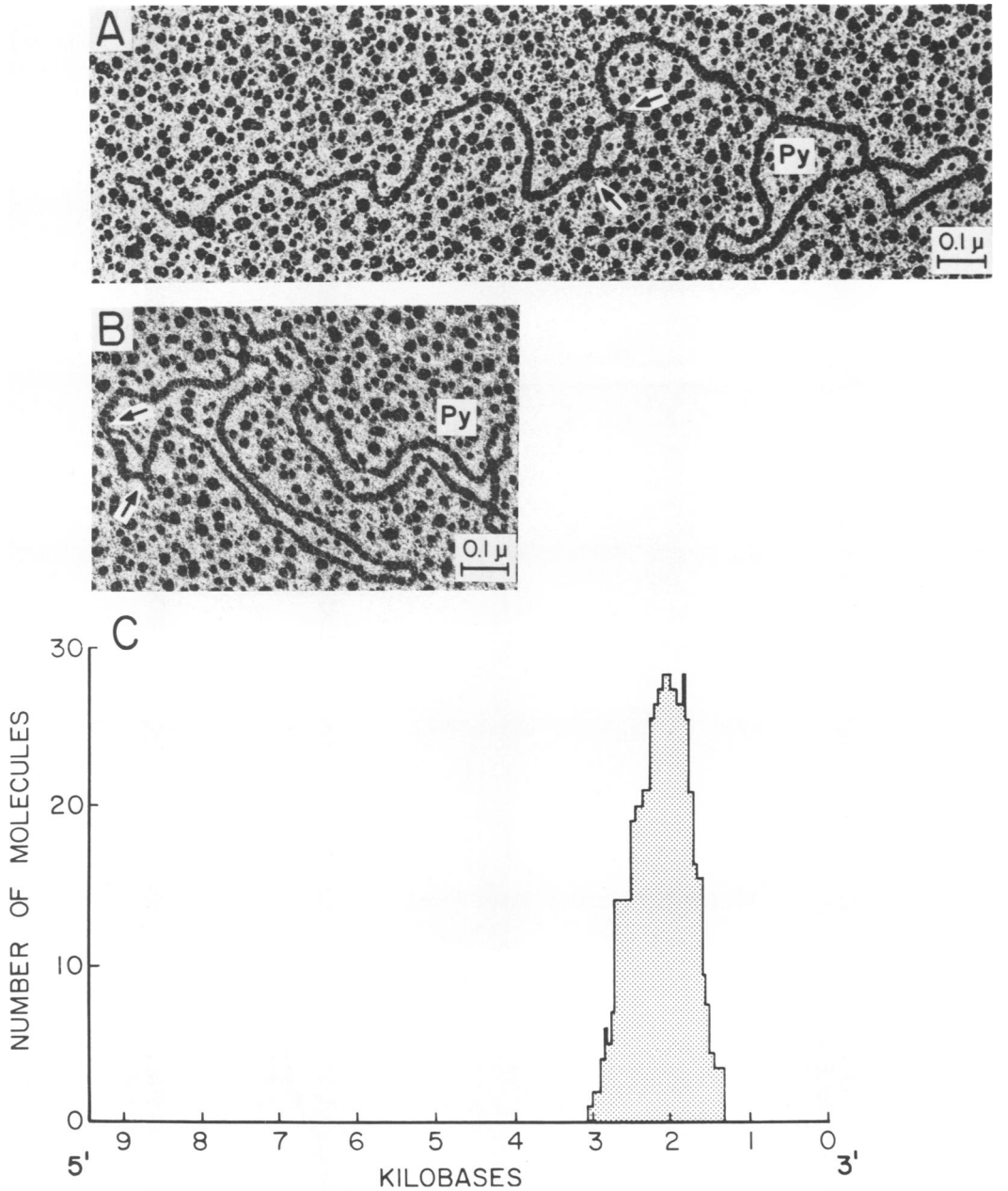

FIG. 1. *Mo-MLV cDNA-BALB/Mo-MCF$_{81}$ RNA. (A) Linear heteroduplex formed between BALB/Mo-MCF$_{81}$ RNA and Mo-MLV cDNA. (B) Circular heteroduplex formed between BALB/Mo-MCF$_{81}$ RNA and Mo-MLV cDNA. Arrows indicate regions of nonhomology. Py, Polyoma. (C) Histogram denoting the 5′ and 3′ ends of the nonhomology loop observed in heteroduplexes formed between BALB/Mo-MCF$_{81}$ RNA and Mo-MLV cDNA. The number of molecules exhibiting a nonhomology loop is plotted against the position of the nonhomology relative to the 3′ end of the genome.*

Mo thymoma lines. To ensure that the cloned isolate Mo-MCF$_{81}$ had not acquired or lost nucleotide sequences during cocultivation or subsequent passaging, virions produced directly by cells of thymoma line Th$_{16.3}$ were purified, and heteroduplexes between Mo-MLV cDNA and Th$_{16.3}$ virion RNA were analyzed.

Vogt (32) has shown recently that the lymphoma-derived Th$_{16.3}$ cell line produces both ecotropic Mo-MLV and dual-tropic Mo-MCF in

a ratio of about 5:1. Thus, we would expect two types of structures, (i) heteroduplexes formed between Mo-MCF component(s) of $Th_{16.3}$ RNA and Mo-MLV cDNA, and (ii) homoduplexes formed between ecotropic Mo-MLV RNA of the $Th_{16.3}$ and Mo-MLV cDNA. Figure 2A shows a typical heteroduplex with a single nonhomology region extending 1.75 ± 0.25 to 2.53 ± 0.33 kb

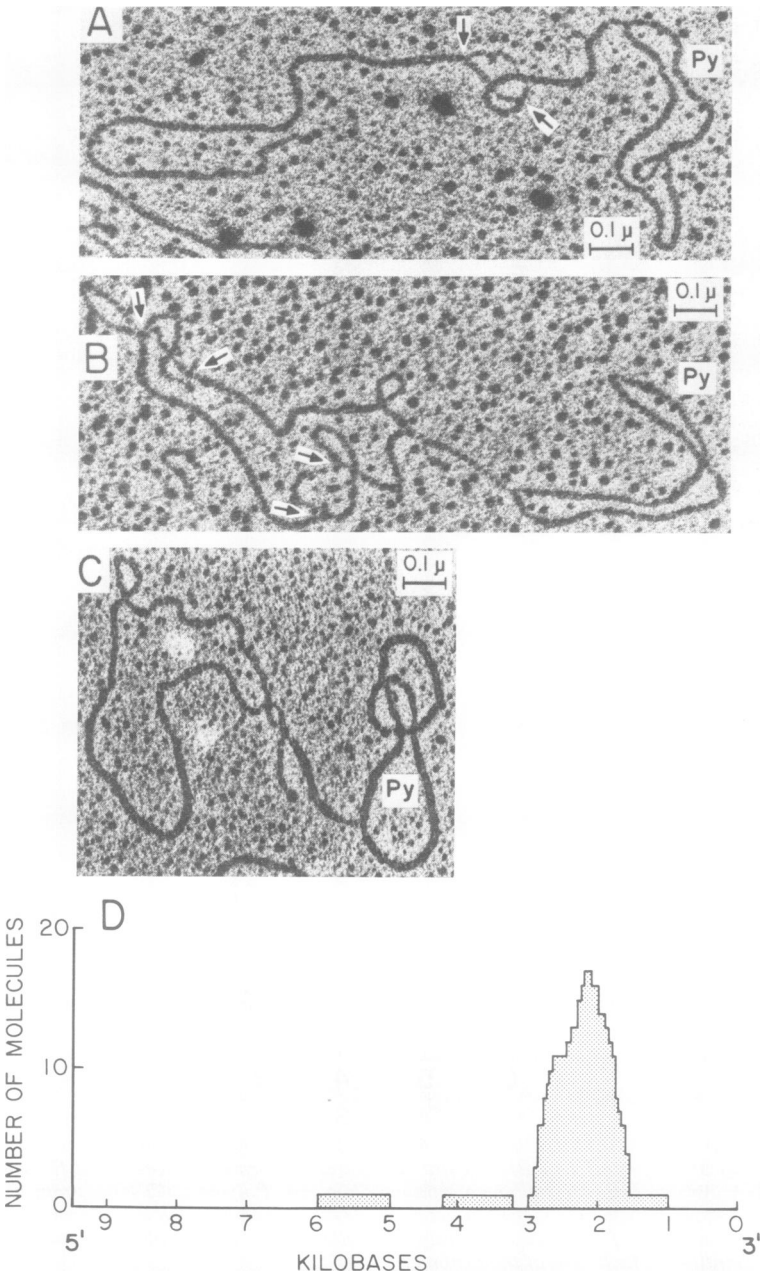

FIG. 2. *Mo-MLV cDNA–virion RNA obtained from $Th_{16.3}$. (A) Linear heteroduplex formed between Mo-MLV cDNA and virion RNA obtained from $Th_{16.3}$. Arrows indicate regions of nonhomology. Py, Polyoma. (B) Circular heteroduplex formed between Mo-MLV cDNA and viral RNA from $Th_{16.3}$. (C) Linear homoduplex formed between the ecotropic component (Mo-MLV) of $Th_{16.3}$ viral RNA and Mo-MLV cDNA. (D) Histogram of coordinates of the nonhomology observed in heteroduplexes formed between $Th_{16.3}$ viral RNA and Mo-MLV cDNA. The number of molecules exhibiting a nonhomology is plotted against the position of the nonhomology relative to the 3′ end of the genome.*

from the 3′ end of the genome. This substitution loop appears to be similar to that shown in Fig. 1A. Although molecules showing substitution loop α appear to be the predominant species of RNA obtained from $Th_{16.3}$, there are other molecules with additional substitution loops distinct from the α substitution loop (Fig. 2B). The distribution of the substitution loops observed in the heteroduplexes formed between Mo-MLV cDNA and virion RNA obtained from $Th_{16.3}$ are shown in a histogram (Fig. 2D).

Approximately 20% of the molecules observed contained at least one substitution loop. The remaining 80% of the molecules showed complete homology and probably represent homoduplexes formed between ecotropic Mo-MLV RNA present in virions obtained from $Th_{16.3}$ and Mo-MLV cDNA transcripts (Fig. 2C). This is in accordance with the biological behavior of the viruses obtained from $Th_{16.3}$ (32).

Localization of xenotropic sequences of Mo-MCF. (i) Mo-MLV cDNA-NZB xenotropic RNA. We were interested in identifying the xenotropic viral sequences present in recombinant envelope genes of Mo-MCF virus. The tryptic peptide maps of gp70 from AKR MCF and Friend MCF viruses showed a peptide spot specific for xenotropic virus (8, 30). In both cases the xenotropic gp70 analyzed was obtained from spontaneously released NZB xenotropic virus. Both a linear heteroduplex and a circular heteroduplex formed between Mo-MLV cDNA and 35S RNA from NZB virions are shown in Fig. 3A and B. Four major regions of nonhomology resulting in substitution loops 1 to 4 can be identified. Figure 3C shows a histogram derived from heteroduplexes formed between Mo-MLV cDNA and 35S NZB RNA. It also tabulates the positions of these substitution loops with respect to the 3′ end of the genome, their lengths, and the percentage of molecules actually exhibiting each loop.

The circular heteroduplex shown in Fig. 3B indicates that Mo-MLV and NZB virus share homologous sequences at the 5′ ends of their genomic RNAs. The region of nonhomology extending 3.62 ± 0.44 to 4.21 ± 0.57 kb can be either a sequence in the *pol* gene or a set of sequences between the *pol* and *env* genes. The substitution loop 4 extending from 7.46 ± 0.7 to 7.92 ± 0.77 kb most likely lies in the *gag* gene. We conclude that there is an extensive nonhomology between the Mo-MLV and NZB virus genomes. However, the 5′ and 3′ termini of the two viral genomic RNAs may share a large sequence homology.

(ii) Mo-MCF cDNA-NZB xenotropic RNA. If the MCF-specific sequences in Mo-MCF RNA are contributed by NZB-like xenotropic RNA, then in a heteroduplex formed between NZB RNA and Mo-MCF cDNA, the MCF-specific substitution loop α will appear as a homologous duplex region. Because of the relative paucity of the availability of large amounts of purified virions from cloned $Mo\text{-}MCF_{81}$, we obtained purified virions from two thymoma lines, $Th_{16.3}$ and $MPV_{11.1}$ (see above), to synthesize large cDNA transcripts. These cell lines produce both Mo-MCF and ecotropic Mo-MLV (32; Vogt, unpublished data). Thus, hybrids formed between long cDNA transcripts and NZB RNA should yield two types of heteroduplexes, one between NZB RNA and Mo-MCF cDNA and the other between NZB RNA and Mo-MLV cDNA. Figures 4A and B show the two types of linear heteroduplexes formed between NZB RNA and Mo-MCF cDNA. Figure 4A shows substitution loops corresponding to substitution loops 1 and 3 shown in Fig. 3C. However, the region of substitution loop 2 which encompasses the MCF-specific substitution loop α appears to be a duplex region. In contrast, Fig. 4B shows the three main substitution loops seen in a heteroduplex formed between Mo-MLV cDNA and 35S NZB RNA. Since the Mo-MCF virions obtained from either $Th_{16.3}$ or $MPV_{11.1}$ contain both ecotropic and MCF Mo-MLV, we conclude that the heteroduplex shown in Fig. 4A represents a hybrid formed between Mo-MCF cDNA and NZB RNA, whereas Fig. 4B shows a heteroduplex formed between ecotropic cDNA and NZB RNA. About 20% of the heteroduplexes scored conformed to Fig. 4A, and the remaining 80% appeared to be of the type shown in Fig. 4B. This ratio is consistent with the biological ratio of the two components (32).

The striking feature of Fig. 4A is the absence of substitution loop α and the appearance of a duplex region instead. The relative positions of substitution loops 1 and 3 seen in a heteroduplex formed between Mo-MLV cDNA and NZB RNA (Fig. 4B) appear to remain unchanged. The average length of the Mo-MCF cDNA transcripts used in these heteroduplexes was about 8.0 ± 1.4 kb. Figure 4C shows a histogram of a number of heteroduplexes formed between Mo-MCF cDNA and NZB RNA. The distribution of substitution loops observed in heteroduplexes formed between Mo-MLV cDNA and NZB RNA was similar to the distribution shown in Fig. 3C.

Sequence relationship of the genomes of BALB-2 and NZB xenotropic viruses. Relatively little was known about the nucleic acid sequence homology of NZB and BALB-2 xenotropic viral genomes (1, 5). We decided to compare the genome organizations of NZB xenotropic and BALB-2 viruses by heteroduplex

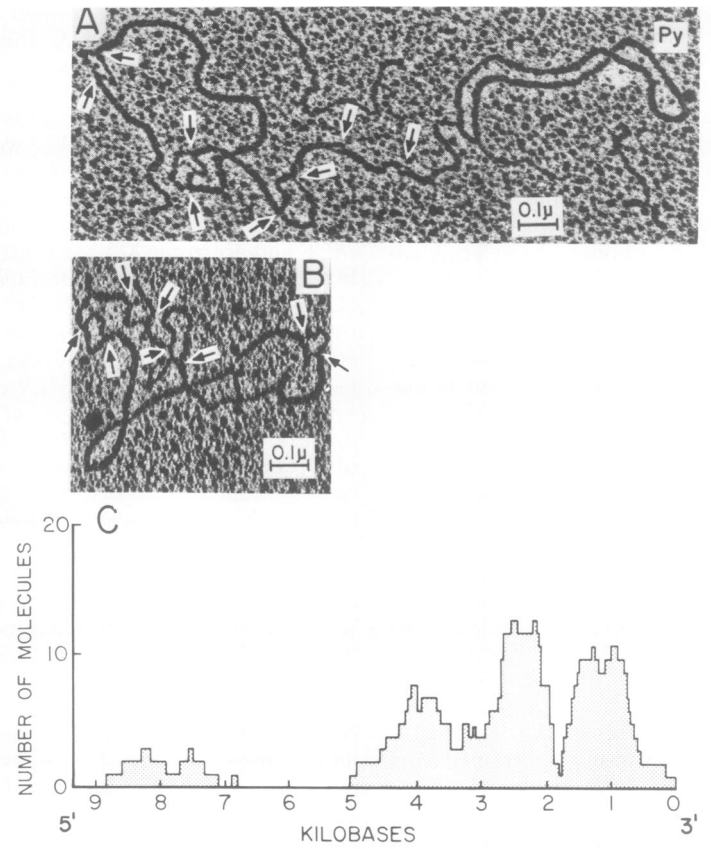

Substitution Loop	Extent of Substitution from 3'→5' (kb)	Average size of the Substitution Loop (kb)	% molecules exhibiting Substitution Loop
1	0.73 ± 0.29 to 1.46 ± 0.35	0.72 ± 0.33	76
2	2.04 ± 0.16 to 2.80 ± 0.30	0.74 ± 0.27	86
3	3.62 ± 0.44 to 4.21 ± 0.57	0.60 ± 0.19	67
4	7.46 ± 0.70 to 7.92 ± 0.77	0.50 ± 0.41	41

FIG. 3. *Mo-MLV cDNA–NZB xenotropic RNA. (A) Linear heteroduplex formed between Mo-MLV cDNA and NZB xenotropic viral RNA. Arrows indicate regions of nonhomology. Py, Polyoma. (B) Circular heteroduplex formed between Mo-MLV cDNA and NZB xenotropic viral RNA. (C) Histogram of coordinates of the nonhomology observed in heteroduplexes formed between Mo-MLV cDNA and NZB xenotropic viral RNA. The number of molecules exhibiting a nonhomology is plotted against the position of the nonhomology relative to the 3' end of the genome. (D) Positions, lengths, and percentages of molecules exhibiting nonhomology loops 1 to 4 observed in heteroduplexes formed between Mo-MLV cDNA and NZB xenotropic viral RNA (A).*

analysis. Of the 29 heteroduplexes formed between BALB-2 cDNA and NZB RNA, 24 appeared to be completely homologous (Fig. 5A). The remaining five molecules showed a single region of nonhomology extending 3.20 ± 0.82 to 3.83 ± 0.74 kb from the 3' end of the genome. One such heteroduplex is shown in Fig. 5B. The average size of the substitution loop varied con-

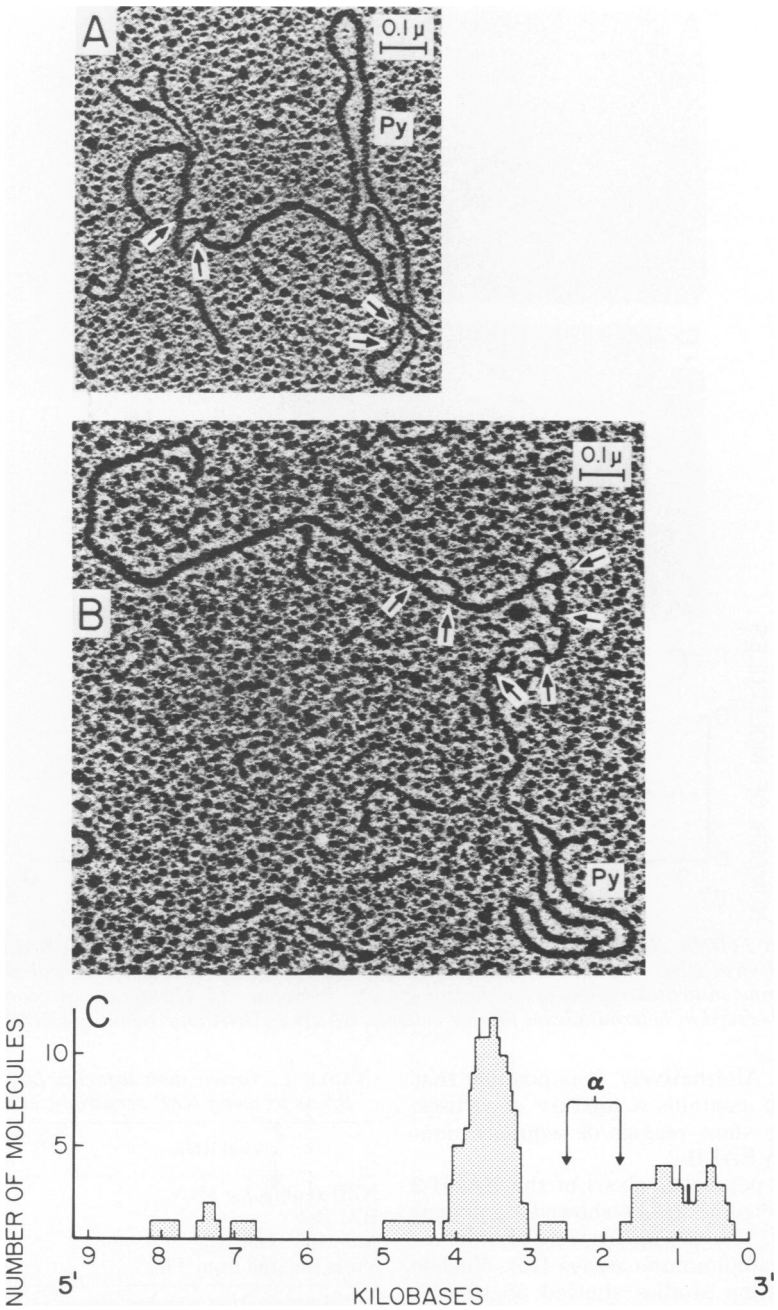

FIG. 4. *Mo-MCF cDNA-NZB xenotropic viral RNA. (A) Linear heteroduplex formed between Mo-MCF cDNA and NZB xenotropic RNA. Arrows indicate regions of nonhomology. Py, Polyoma. (B) Linear heteroduplex formed between NZB xenotropic viral RNA and the ecotropic component (Mo-MLV) of Mo-MCF cDNA. (C) Histogram of coordinates of the nonhomology observed in heteroduplexes formed between NZB xenotropic viral RNA and Mo-MCF cDNA.*

siderably and appeared to be 0.72 ± 0.51 kb. A histogram presenting the range of the sizes of the substitution loop is shown in Fig. 5C. The wide variations in the position and size of the substitution loop, coupled with the relatively low frequency at which they are observed, suggest a large degree of sequence homology between the genomes of NZB and BALB-2 xeno-

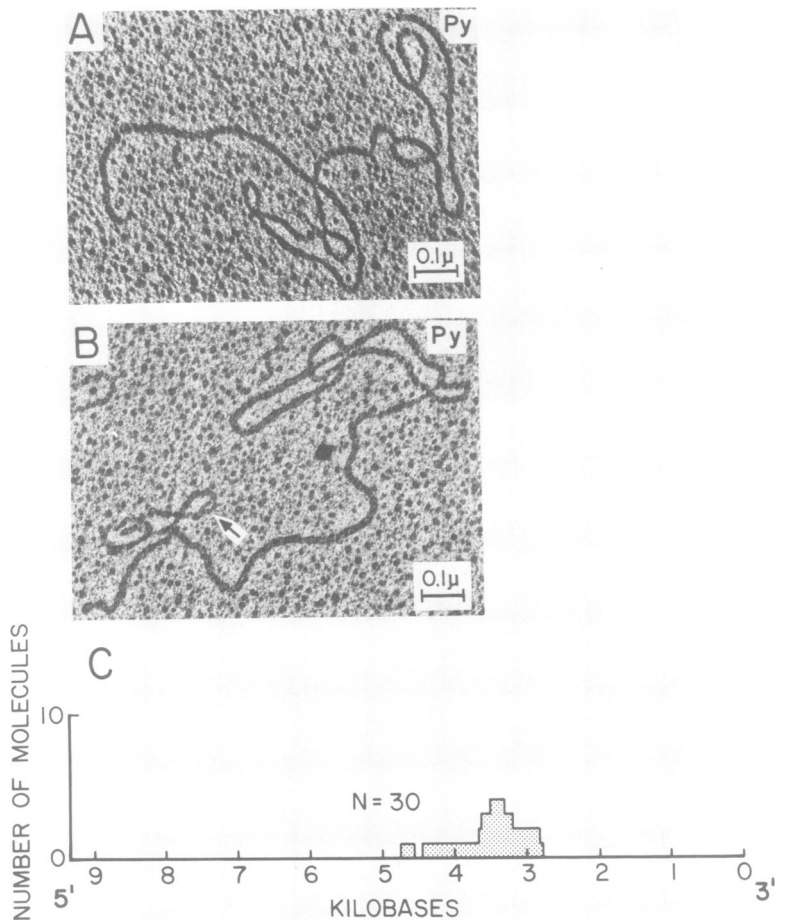

FIG. 5. *BALB-2 cDNA-NZB xenotropic RNA. (A) Linear homoduplex formed between BALB-2 cDNA and xenotropic NZB viral RNA. (B) Linear heteroduplex formed between BALB-2 cDNA and xenotropic NZB viral RNA. Arrow indicates region of nonhomology. Py, Polyoma. (C) Histogram of coordinates of the nonhomology observed in heteroduplexes formed between BALB-2 cDNA and xenotropic NZB viral RNA.*

tropic viruses. Alternatively, it is possible that the NZB virus contains a mixture of viruses, some of which show regions of sequence nonhomology with BALB-2.

The tryptic peptide analysis of the BALB-2 and NZB xenotropic gp70's showed significant differences (9). The two gp70's were also distinguishable by radioimmune assays (19). Nucleic acid hybridization studies showed 55 to 65% sequence homology (5). To confirm our results of heteroduplex analysis, we also performed nucleic acid hybridization experiments. We synthesized cDNA from purified NZB xenotropic viruses and hybridized it to various viral RNAs. Table 1 summarizes these results. The 35S BALB-2 RNA appears to hybridize about 80% to NZB cDNA. This is consistent with the heteroduplex data showing large homology between the two viral genomes. The heteroduplex criterion is less stringent than S1 nuclease digestion and is unable to distinguish 10 to 20% base pair mismatch. Table 1 also shows a 50% sequence homology between ecotropic Mo-MLV RNA and NZB xenotropic cDNA. This is in general

TABLE 1. *Nucleic acid sequence homology of viral RNAs by using NZB xenotropic cDNA as probe*

Viral RNA	% of hybridization to NZB cDNA[a]
NZB xenotropic MLV	100
BALB-2	79
Mo-MLV clone E7	50
Virus isolated from $Th_{16.3}$	66

[a] Hybridization was performed as described in the text. Hybridization values were normalized and were corrected for 10 to 15% self-annealing and for maximum hybridization of 80 to 90%. In the case of BALB-2, 35S viral RNA was isolated by sucrose gradient centrifugation after denaturation of the RNA by incubation as described previously (20).

agreement with the heteroduplex data, which show an overall sequence nonhomology of about 30 to 40%. Hybridization of NZB cDNA to virion RNA obtained from $Th_{16.3}$ showed sequence homology greater than that observed with Mo-MLV RNA. This increase can be partially accounted for by the presence of xenotropic sequences in the Mo-MCF RNA component of $Th_{16.3}$ RNA.

DISCUSSION

BALB/Mo-MCF is an *env* gene recombinant. Heteroduplexes formed between BALB/Mo-MCF RNA obtained from either a cloned isolate or a primary tumor cell line and Mo-MLV cDNA show a single nonhomology region (substitution loop α; Fig. 1 and 2) of approximately 0.7 ± 0.18 kb. The substitution loop α extends 1.7 to 2.4 kb from the 3′ end of the genome. The extent and location of the substitution loop α found in Mo-MCF RNA is similar to those described for AKR MCF 247, Mo-MCF_{83}, and HIX viral RNAs (5, 6). Although other substitution loops were observed (Fig. 2B), the major substitution loop in heteroduplexes formed between RNA from virions obtained from the thymoma cell line and Mo-MLV cDNA is identical to that obtained from RNA of a cloned isolate. Thus, it appears that Mo-MCF_{81} is a cloned isolate of a predominant species occurring in the primary tumor cell line. The significance of the other substitution loops observed in Fig. 2B remains unclear.

It has been shown that the *env* gene of Mo-MLV is about 2.7 to 3.0 kb long and is located at the 3′ end of the genome (7, 13). Based upon the heteroduplex data, it appears that the N terminus of the major glycoprotein of dual-tropic Mo-MCF is contributed by the xenotropic virus, whereas the carboxy terminus is similar to that of the parental ecotropic virus. It is, however, possible that duplex regions formed on either side of substitution loop α are not entirely homologous. The heteroduplex techniques employed here cannot distinguish duplexes involving 10 to 20% base pair mismatches.

BALB/Mo-MCF-specific sequences are related to xenotropic viruses. We were interested in determining the parent xenotropic virus involved in recombination to form Mo-MCF obtained from a cloned isolate or a primary tumor. The results shown in Fig. 4 indicate an absence of substitution loop α in a heteroduplex formed between NZB RNA and Mo-MCF cDNA, whereas the other substitution loops observed in a heteroduplex between NZB RNA and Mo-MLV cDNA (Fig. 3) can still be visualized. Thus, it appears that NZB RNA contains sequences analogous to the MCF-specific α substitution loop. The presence of substitution loop 3 in Fig. 4 suggests that other regions of nonhomology between xenotropic NZB RNA and ecotropic MLV RNA (Fig. 3) are maintained. It should, however, be pointed out that the duplex structures seen in Fig. 4 do not rule out yet other regions of recombination between ecotropic Mo-MLV and xenotropic viruses. For instance, a region of homology seen in Fig. 3 between NZB RNA and Mo-MLV cDNA also appears as a region of homology in a heteroduplex formed between NZB RNA and Mo-MCF cDNA.

Relationship of NZB virus and BALB-2. The serum of many mouse strains contains a gp70 similar to that expressed by NZB virus (9). Elder et al. (9) have shown, on the basis of tryptic peptide maps, that the gp70's of BALB-2 and NZB xenotropic virus are quite distinct. Hino et al. (19) have also classified BALB-2 and NZB virus into separate classes by radioimmune assays. Nucleic acid hybridization studies (5) have shown a sequence homology of 50 to 60% between the two viruses. The hybridization results presented in Table 1 show a sequence homology of about 80%. The heteroduplex data suggest that the genomes of the two viruses are highly related. The only region of nonhomology detected extended 3.2 ± 0.82 to 3.83 ± 0.74 kb from the 3′ end of the genome. This region is outside the *env* gene (7) and may represent either the *pol* gene or intergene sequences. Tryptic peptide maps are, however, a very sensitive method, and a single base change can alter the pattern. Sensitive techniques like the S1 mapping procedure of Berk and Sharp (4) and T1 oligonucleotide finger-printing can resolve the issue of sequence homology between the two viral genomes more satisfactorily.

Our inability to distinguish between the *env* gene sequences of BALB-2 and NZB xenotropic virus by heteroduplex formation leaves open the question of which xenotropic viral sequences are involved in the formation of recombinant Mo-MCF viruses. We are trying to approach this question by determining the nucleotide sequences of cloned segments of the *env* gene of Mo-MCF, NZB, and BALB-2 viruses.

ACKNOWLEDGMENTS

We are very grateful to N. Davidson and Y. Chien, California Institute of Technology, for teaching us the heteroduplex techniques. We thank Rudolf Jaenisch, Fred Jensen, and Bob Hyman for various materials. We thank Billie Green, Susan Swift, Marianne McKennett, and Candy Haggblom for technical assistance. We thank J. T. Simon and C. Goller for help in preparing the manuscript.

L.J.L.D.V. was supported by a grant from the Niels Stensen Foundation, Amsterdam, The Netherlands. This work was supported by Public Health Service grants CA 16561, CA 21408, and CA 3608-06A1 from the National Cancer Institute.

LITERATURE CITED

1. **Aaronson, S. A., and J. R. Stephenson.** 1973. Independent segregation of loci for activation of biologically distinguishable RNA C-type viruses in mouse cells. Proc. Natl. Acad. Sci. U.S.A. **70**:2055-2058.
2. **Bender, W., and N. Davidson.** 1976. Mapping of poly(A) sequences in the electron microscope reveals unusual structure of type C oncornavirus RNA molecules. Cell **7**:595-607.
3. **Benveniste, R. E., M. M. Lieber, and G. J. Todaro.** 1976. A distinct class of inducible murine type C viruses that replicates in the rabbit SIRC cell line. Proc. Natl. Acad. Sci. U.S.A. **71**:602-606.
4. **Berk, A. J., and P. A. Sharp.** 1978. Structure of the adenovirus 2 early mRNAs. Cell **14**:695-711.
5. **Callahan, R., M. M. Lieber, and G. Todaro.** 1975. Nucleic acid homology of murine xenotropic type C viruses. J. Virol. **15**:1378-1384.
6. **Chien, Y.-H., I. M. Verma, T. Y. Shih, E. M. Scolnick, and N. Davidson.** 1978. Heteroduplex analysis of the sequence relations between the RNAs of mink cell focus-inducing and murine leukemia viruses. J. Virol. **28**:352-360.
7. **Donoghue, D. J., E. Rothenberg, N. Hopkins, D. Baltimore, and P. A. Sharp.** 1978. Heteroduplex analysis of the non-homology region between Moloney MuLV and the dual host range derivative HIX virus. Cell **14**: 959-970.
8. **Elder, J. H., J. W. Gautsch, F. C. Jensen, R. A. Lerner, J. W. Hartley, and W. P. Rowe.** 1977. Biochemical evidence that MCF murine leukemia viruses are envelope (env) gene recombinants. Proc. Natl. Acad. Sci. U.S.A. **74**:4676-4680.
9. **Elder, J. H., F. C. Jensen, M. L. Bryant, and R. A. Lerner.** 1977. Polymorphism of major envelope glycoprotein (gp70) of murine C-type viruses: virion associated and differentiation antigens coded by multigene family. Nature (London) **267**:23-28.
10. **Faller, D. V., J. Rommelaere, and N. Hopkins.** 1978. The large T_1-oligonucleotides of Moloney murine leukemia virus that are missing in an env gene recombinant, HIX are present on an intracellular 21S Moloney viral RNA. Proc. Natl. Acad. Sci. U.S.A. **75**:2964-2968.
11. **Fan, H., and D. Baltimore.** 1973. RNA metabolism of murine leukemia virus: detection of virus-specific RNA sequences in infected and uninfected cells and identification of virus-specific messenger RNA. J. Mol. Biol. **83**:93-117.
12. **Fan, H., and M. Paskind.** 1974. Measurement of the sequence complexity of cloned Moloney murine leukemia virus 60 to 70S RNA: evidence for a haploid genome. J. Virol. **14**:421-429.
13. **Fan, H., and I. M. Verma.** 1978. Size analysis and relationship of murine leukemia virus-specific mRNA's: evidence for transposition of sequences during synthesis and processing of subgenomic mRNA. J. Virol. **26**:468-478.
14. **Fischinger, P. J., J. N. Ihle, F. de Noronha, and D. P. Bolognesi.** 1977. Oncogenic and immunogenic potential of cloned HIX virus in mice and cats. Med. Microbiol. Immunol. **164**:119-129.
15. **Fischinger, P. J., S. Nomura, and D. P. Bolognesi.** 1975. A novel murine oncornavirus with dual eco- and xenotropic properties. Proc. Natl. Acad. Sci. U.S.A. **72**: 5150-5155.
16. **Gross, L.** 1970. Oncogenic viruses. Pergamon Press Ltd., London.
17. **Hartley, J. W., and W. P. Rowe.** 1976. Naturally occurring murine leukemia viruses in wild mice: characterization of a new "amphotropic" class. J. Virol. **19**:19-25.
18. **Hartley, J. W., N. K. Wolford, L. J. Old, and W. P. Rowe.** 1977. A new class of murine leukemia virus associated with development of spontaneous lymphomas. Proc. Natl. Acad. Sci. U.S.A. **74**:789-792.
19. **Hino, S., J. R. Stephenson, and S. A. Aaronson.** 1976. Radioimmune assays for the 70,000-molecular-weight glycoproteins of endogenous mouse type C viruses: viral antigen expression in normal mouse tissues and sera. J. Virol. **18**:933-941.
20. **Hu, S., N. Davidson, and I. M. Verma.** 1977. A heteroduplex study of the sequence relationships between the RNAs of M-MSV and M-MLV. Cell **10**:469-477.
21. **Jaenisch, R.** 1976. Germ line integration and Mendelian transmission of the endogenous Moloney leukemia virus. Proc. Natl. Acad. Sci. U.S.A. **73**:1260-1264.
22. **Jaenisch, R.** 1977. Germ line integration of Moloney murine leukemia virus: effect of homozygosity of the M-MuLV locus. Cell **12**:691-696.
23. **Levy, J.** 1973. Xenotropic viruses: murine leukemia viruses associated with NIH Swiss, NZB and other mouse strains. Science **182**:1151-1153.
24. **Rasheed, S., M. B. Gardner, and E. Chan.** 1976. Amphotropic host range of naturally occurring wild mouse leukemia viruses. J. Virol. **19**:13-18.
25. **Rommelaere, J., D. V. Faller, and N. Hopkins.** 1978. Characterization and mapping of RNase T_1 resistant oligonucleotides derived from the genomes of AKV and MCF murine leukemia viruses. Proc. Natl. Acad. Sci. U.S.A. **75**:495-499.
26. **Shih, T. Y., M. O. Weeks, D. H. Troxler, J. M. Coffin, and E. M. Scolnick.** 1978. Mapping host range-specific oligonucleotides within genomes of the ecotropic and mink cell focus-inducing strains of Moloney murine leukemia virus. J. Virol. **26**:71-83.
27. **Taylor, J.** 1977. An analysis of the role of tRNA species as primers for the transcription into DNA of RNA tumor virus genomes. Biochim. Biophys. Acta **473**:57-71.
28. **Taylor, J. M., R. Illmensee, and J. Summers.** 1976. Efficient transcription of RNA into DNA by avian sarcoma virus polymerase. Biochim. Biophys. Acta **442**: 324-330.
29. **Troxler, D. H., and E. M. Scolnick.** 1978. Rapid leukemia induced by cloned Friend strain of replicating murine type-C virus: association with induction of xenotropic-related RNA sequences contained in spleen focus forming virus. Virology **85**:17-27.
30. **Troxler, D. H., E. Yuan, D. Linemeyer, S. Ruscetti, and E. M. Scolnick.** 1978. Helper independent mink cell focus-inducing strains of Friend murine type-C virus: potential relationship to the origin of replication-defective spleen focus-forming virus. J. Exp. Med. **148**: 639-653.
31. **Verma, I. M.** 1978. Genome organization of RNA tumor viruses. I. In vitro synthesis of full-genome-length single-stranded and double-stranded viral DNA transcripts. J. Virol. **26**:615-629.
32. **Vogt, M.** 1979. Properties of "mink cell focus-inducing" (MCF) virus isolated from spontaneous lymphoma lines of BALB/c mice carrying Moloney murine leukemia virus as an endogenous virus. Virology **93**: 226-236.